Suppression of enteroendocrine cell glucagon-like peptide (GLP)-1 release by fat-induced small intestinal ketogenesis; a mechanism targeted by Roux-en-Y Gastric Bypass surgery but not by preoperative Very-Low-Calorie Diet

Short title: Gastric bypass decreases intestinal ketogenesis

Ville Wallenius*[1], Erik Elias[1], Erik Elebring[1], Bauke Haisma[2], Anna Casselbrant[1], Pierre Larraufie[2], Emma Spak[1], Frank Reimann[2], Carel W. le Roux[1,3], Neil G. Docherty[1,3], Fiona M. Gribble[2], Lars Fändriks[1].

[1]Department of Gastrosurgical Research and Education, Sahlgrenska Academy, University of Gothenburg, Gothenburg, Sweden. [2]Metabolic Research Laboratories, University of Cambridge, Cambridge, United Kingdom, [3]Diabetes Complications Research Centre, Conway Institute, University College of Dublin, Dublin, Ireland.

* Corresponding Author:
Ville Wallenius, Associate Professor, PhD, MD.
Department of Gastrosurgical Research and Education, Sahlgrenska Academy, University of Gothenburg, Vita stråket 12, SE-413 45 Gothenburg, Sweden.
Email: ville.wallenius@gastro.gu.se
Phone: +46 (0) 733 836749

Keywords: bariatric surgery; Roux-en-Y gastric bypass; proteomic; global protein expression; small intestine; mucosa; jejunum; Roux-limb; alimentary limb; mitochondrial 3-hydroxy-3-methylglutaryl-CoA synthase; mHMGCS; ketone bodies; β-hydroxybutyrate; glucagon-like peptide-1.

List of abbreviations

RYGB=Roux-en-Y gastric bypass, EEC=enteroendocrine cell,

GLP-1=glucagon-like peptide-1, VLCD=very-low calorie diet, HFD=high-fat diet,

LFD=low-fat diet, mHMGCS=mitochondrial 3-hydroxy-3-methylglutaryl-CoA synthase,

βHB=β-hydroxybutyrate, GAPDH=Glyceraldehyde-3-phosphate dehydrogenase,

IBMX=3-isobutyl-1-methylxanthine, PTX=pertussis toxin, SEM=standard error of the mean.

Word count: 4000

ABSTRACT

Objective: Food intake normally stimulates release of satiety and insulin-stimulating intestinal hormones, such as glucagon-like peptide (GLP)-1. This response is blunted in obese insulin resistant subjects, but is rapidly restored following Roux-en-Y gastric bypass (RYGB) surgery. We hypothesized this a result of the metabolic changes taking place in the small intestinal mucosa following the anatomical rearrangement after RYGB surgery, and aimed at identifying such mechanisms.

Design: Jejunal mucosa biopsies from patients undergoing RYGB surgery were retrieved at time of operation, before and after very-low calorie diet, and 6 months postoperatively. Samples were analyzed by global protein expression analysis and Western blotting. Biological functionality of these findings was explored in mice and primary jejunal cell cultures.

Results: The most prominent change found after RYGB was decreased jejunal expression of the rate-limiting ketogenic enzyme mitochondrial 3-hydroxy-3-methylglutaryl-CoA synthase (mHMGCS), corroborated by decreased ketone body levels. In mice, prolonged high-fat feeding induced the expression of mHMGCS and functional ketogenesis in jejunum. The effect of ketone bodies on gut peptide secretion was subsequently tested on enteroendocrine cells (EECs) in mouse primary jejunal cultures, where a ~40% inhibition of GLP-1 release was found compared to baseline.

Conclusion: Intestinal ketogenesis is induced by high-fat diet and inhibited by RYGB surgery. In cell culture, ketone bodies inhibited GLP-1 release from EECs. Thus, we suggest that this may be a mechanism by which RYGB can remove the inhibitory effect of ketone bodies on EECs, thereby restituting the responsiveness of EECs resulting in increased meal-stimulated levels of GLP-1 after surgery.

Summary box

1. What is already known about this subject?

   Roux-en-Y Gastric Bypass surgery for obesity has rapid, non-weight-dependent effects on glucose metabolism that cannot be explained by perioperative starvation alone.

2. What are the new findings?

   Intestinal ketogenesis, induced by prolonged high-fat feeding, may be a mechanism blunting GLP-1 responsiveness in obese subjects before surgery. After Gastric Bypass-surgery, this mechanism may be relieved by the inhibition of intestinal ketogenesis, promoting the rapid improvement of the GLP-1 response after surgery.

3. How might it impact on clinical practice in the foreseeable future?

   It may be possible to pharmaceutically target intestinal ketogenesis and thereby counteract the diabetogenic effect of obesity without the need for Gastric Bypass surgery.

INTRODUCTION

Roux-en-Y gastric bypass (RYGB) is effective in long-term treatment of morbid obesity and type-2 diabetes [1]. Weight loss *per se* is an important factor behind the improved metabolic state, but RYGB also activates early postoperative weight-independent mechanisms, for example the meal-induced release of gut peptides [2, 3]. Such RYGB associated effects have highlighted the effects of the anatomical reconfiguration of the alimentary tract in whole-body metabolism. Therefore, we used RYGB as a model to try to find novel intestinal-associated mechanisms in the proximal small intestine to improved glucose metabolism.

Following RYGB the former midgut jejunum becomes the alimentary limb anastomosed to a 30ml gastric pouch at the esophagogastric junction. Food has to pass 1.5 m in the alimentary limb to the jejuno-jejunostomy before enzymatic digestion starts. Surprisingly small changes occur in the morphological appearance of the jejunal mucosa of the alimentary limb [4, 5]. However, functional studies suggest that the digestion-deprived alimentary limb fails to assimilate luminal glucose [6-8]. Apparently, it undergoes an induction of glucose uptake from the blood circulation, potentially with a glycemia lowering effect [8, 9]. It is likely that pre-processing of triglycerides by bile and gastric and pancreatic lipase is deficient. Therefore, food digestion and nutrient-absorption become localized mainly to the distal jejunum and ileum. Increased stimulation of enteroendocrine cells (EECs) by undigested food in the distal small intestine has been suggested as the main mechanism causing the augmented release of enteroendocrine gut peptides e. g. gastric inhibitory peptide, peptide YY and glucagon-like peptide-1 (GLP-1). As additional theory, it has been suggested that preventing exposure of proximal gastrointestinal tract to food could inhibit the release of a hitherto unknown “anti-incretin” factor that reduces insulin release or decreases insulin sensitivity, and its demise could explain the rapid improvement of gut-peptide release and glucose

metabolism after RYGB surgery [9, 10]. The present study was initiated in order to search for such novel glucose-lowering mechanisms after RYGB.

MATERIALS AND METHODS

Surgery and patients

Anthropometric characteristics of the patient pilot study cohorts are shown in Table 1. Patients in the proteomics cohort either underwent primary RYGB (4 patients) or a conversion from vertical banded gastroplasty to RYGB (3 patients). In the confirmatory cohort, 9 patients were included, 8 of whom underwent a primary RYGB and one underwent conversion from vertical banded gastroplasty to RYGB. In the diet cohort, 12 patients were recruited to also include mucosa sampling before the start of the two-week very-low-calorie diet (VLCD) preceding RYGB surgery. Samples were retrieved as previously described [5]. In brief, during RYGB surgery, a few centimeters of the jejunum 50-60 cm distal to ligament of Treitz was retrieved for research purposes when omega-loop, between the gastro-enterostomy and the jejuno-jejunostomy, was divided to create the final Roux-en-Y construction (Supplementary Figure 1A, left panel). The mucosa/submucosa was separated from the musculature by sharp dissection. Before surgery in the diet cohort, and six to eight months after surgery in all cohorts, patients underwent an endoscopic examination of the jejunum/Roux limb to retrieve mucosa samples (Supplementary Figure 1A, right panel). All endoscopies were performed for research purposes. Mucosal tissue specimens were snap-frozen in liquid nitrogen and kept frozen at -70°C. In these pilot studies, the number of patients included was arbitrarily based on estimations of feasibility of samples size in the global proteomics analysis. The confirmatory samples were retrieved from cohorts where all pre-, peri- and postoperative samples were available. This study was approved by the Regional Ethics Review Board of Gothenburg, approval numbers 193-02, 647-05 and 007-09,

and performed in accordance with the Declaration of Helsinki. All patients signed informed consent before inclusion in the study.

Table 1. Patient characteristics in proteomics, confirmation and diet groups.

Patient group	**Proteomics (n=7)**		**Confirmation (n=9)**		**Diet (n=12)**	
Female	4 (57.1%)		7 (77.8%)		8 (66.7%)	
Diabetes	2 (28.6%)		4 (44.4%)		6 (50%)	
Re-gastroplasty	3 (42.9%)		1 (11.1%)		0 (0%)	
	Median	**Average**	**Median**	**Average**	**Median**	**Average**
Age	46	46.0	49	50.4	56.5	52.8
BMI peri-op.	41.6	40.7	40.3	40.3	39.1	39.6
BMI post-op.	30.0	31.3	31.8	31.8	30.3	30.7
BMI change	-8.9	-9.4	-8.8	-8.5	-9.0	-8.9
%EBMIL	66.4	58.9	59.4	58.2	61.9	61.3

BMI=Body mass index (kg/m2)
%EBMIL=Percent excess BMI loss

Global protein expression analysis of human jejunal mucosa

The technique has been described earlier [11]. Only proteins being consistently changed in all patients and with at least a 50% change from baseline were included for further analysis.

Animal studies

Four- to five-week-old male and female C57BL/6J mice were purchased from Harlan (Horst, Netherlands). Animals were maintained under controlled temperature (23°C) and light (lights on, 6:30–18:30 hrs), with *ad libitum* access to water and pelleted food (R34 Lactamin, Kimstad, Sweden) with a nutrient content of g%: fat 4%, protein 16.5%, carbohydrate 58.0%; total calorific content: 3 kcal/g. For HFD experiments, six- to eight-week-old male mice were fed high-fat diet (HFD) or low-fat diet (LFD) for 3 weeks or 3 months. The HFD consisted of

pelleted food (Surwit Diabetogenic Rodent Diet, D12309; Research Diets, New Brunswick, NJ) and had a nutrient content in g%: fat 35.9%, protein 23%, carbohydrate 35.5%; total calorific content: 5.6 kcal/g. The LFD animals continued to receive their usual diet (R34). All animal procedures were approved by the animal ethics committee of the University of Gothenburg, approval numbers 90-2007 and 246-2009.

In the first set of experiments the mice were sacrificed after 3 weeks of either LFD or HFD and different parts of the small intestine; duodenum (proximal 3 cm), jejunum (middle 3 cm) and ileum (distal 3 cm), as well as the liver, were sampled. Full thickness samples of intestinal wall and one liver lobe were snap-frozen in liquid nitrogen and kept frozen (-70°C) for later analysis of protein expression by Western blotting (see below).

In a second set of experiments the mice were fed LFD or HFD for 3 months. On the study day, food was removed for 45 min before experimentation in order to synchronize feeding status. At the start of the experiment an oral gavage with 250 µl of Intralipid® (Soy oil 200 mg/mL, purified egg phospholipids, glycerol, sodium hydroxide, water; Fresenius Kabi, Sweden) was given, containing either vehicle (20 µl of ethyl acetate), 2.5 mg of the mitochondrial 3-hydroxy-3-methylglutaryl-CoA synthase (mHMGCS) inhibitor hymeglusin (Santa Cruz Biotechnology, Santa Cruz, CA; dissolved in vehicle) or 25 mg of β-hydroxybutyrate (βHB, Sigma-Aldrich, St Louis, MO; dissolved in vehicle). At 15, 30 or 120 min, venous blood samples were retrieved from the tail and βHB was analysed using a GlucoMen LX β-ketone sensor (A. Menarini Diagnostics, Firenze, IT).

In a third set of experiments the mice were kept on LFD or HFD for 3 weeks and fasted for 6 hrs before start of the experiment. Then an oral gavage with 500 µl of Intralipid® (Fresenius

Kabi) was given and after an additional 90 min the mice were anaesthetized using isoflurane. A laparotomy was performed and the portal vein was identified and punctured using a thin needle and blood was collected. Peripheral blood samples were concomitantly drawn from the eye. Blood samples were centrifuged to prepare serum. βHB was analysed in serum using an EnzyChrom Ketone Body Assay kit (BioAssay Systems, Hayward, CA).

Biopsy homogenization, Western blotting and βHB quantification

For human confirmatory and diet cohorts, and all murine frozen jejunal mucosa specimens, tissue samples were prepared as described earlier [11]. For proteomics cohort, proteins had already been isolated for global protein expression analysis. For each detected band, density was quantified, and expressed as a percentage of the total densities of all bands of that specific size on the same membrane. Glyceraldehyde-3-phosphate dehydrogenase (GAPDH) was used as loading control. For antibodies please see Supplementary Table 1.

For βHB quantification, tissue homogenates peri- and post-RYGB from the "diet cohort" were analyzed using βHB Colorimetric Assay Kit (Cayman Chemical, Ann Arbor, MI) and results normalized to homogenate protein content.

Histology of human jejunal mucosa

Jejunal mucosal specimens retrieved from patients peri- and post-RYGB (n=5, random selection from confirmatory cohort) were processed according to standard procedures for histology specimen preparation. Briefly, biopsies were fixed in phosphate-buffered 4% formaldehyde, dehydrated and embedded in paraffin. Embedded biopsies were cut in 5 μm sections. For immunofluorescence, sections were rehydrated, antigens were retrieved and sections were blocked in 5% normal goat serum (31872, ThermoFisher Scientific, Rockford,

IL) before incubation with primary antibody overnight at 4°C. Slides were then washed and incubated with secondary antibody for 2 hrs. at room temperature and counter-stained with Hoechst staining (H6024, Sigma-Aldrich). For antibodies please see Supplementary Table 1. Sections with blocking buffer instead of primary antibody were included as negative controls. For general histology, hematoxylin & eosin staining was performed according to standard procedures.

Mouse jejunal primary culture and GLP-1 secretion quantification

Mouse jejunal primary cultures were prepared from mice on C57BL6 background conforming to the UK Home Office project license 70/7824 and local regulations (Animals (Scientific Procedures) Act 1986 Amendment Regulations (SI 2012/3039) as previously described [12]. In brief, the intermediate 10-15 cm region of the small intestine was isolated, digested and crypts were isolated. Crypts were then seeded on Matrigel-coated 24-well plates in high glucose DMEM supplemented with 10% FBS, 2 mM L-Glutamine and 100 U/mL penicillin and 0.1 mg/mL streptomycin and 10 μM Y-27632. The day after plating, cells were washed with saline secretion buffer (138 mM NaCl, 4.5 mM KCl, 4.2 mM $NaHCO_3$, 1.2 mM NaH_2PO_4, 2.6 mM $CaCl_2$, 1.2 mM $MgCl_2$, 10 mM HEPES and 0.1% BSA, pH 7.4) with 1 mM glucose for 30 min. A first hour incubation was performed in secretion buffer with 1 mM glucose, supernatant collected and replaced for a second hour with secretion buffer with different additives: 10 mM glucose + 0.1 mM 3-isobutyl-1-methylxanthine (IBMX), 10 mM glucose + 0.1mM IBMX + 10 mM βHB, 10 mM glucose + 0.1 mM IBMX + 0.1 μM somatostatin. Supernatants were centrifuged for 5 min 1,000 g at 4°C to remove any cell debris and directly snap-frozen until analysis. Samples were analyzed for total GLP-1 (Mesoscale Discovery, Rockville, MD) and data were normalized to the first hour secretion from the same well. Pertussis toxin (PTX, 500 ng/mL), when used, was added to cells 4-5 hrs.

after plating, allowing a 16 hrs. preincubation before the start of the secretion experiment, and was included during the secretion experiment.

Patient and public involvement

The public and patients were not involved in the design, recruitment or conduct of this study.

Statistical analyses

Student's t-test was used for analysis of statistical changes in protein levels in the proteomics analysis of spot intensities on 2D gel electrophoresis. Two-way ANOVA followed by Tukey´s honestly significant difference test was used for analysis of GLP-1 secretion data. Non-parametric Wilcoxon signed-rank test was used for paired human data and non-parametric Mann-Whitney U-test for unpaired mice data. All statistics were performed using Prism 7 and 8 (GraphPad, La Jolla, CA). If not otherwise stated, mean and standard error of the mean (SEM) are presented in figures.

RESULTS

RYGB reduced jejunal mHMGCS protein expression

Intraindividual global protein expression analysis was performed to identify changes in the proteome of human mucosal jejunal biopsies retrieved during operation and 6–8 months postoperatively. In total, 27 protein spots corresponding to 12 unique proteins passed the selection criteria (uni-directionally, regulated by at least 50% from baseline following RYGB). The four protein spots with the strongest down-regulation (mean decrease of -3.8-fold; $P<0.001$) following RYGB were identified by tandem mass spectrometry as mHMGCS. Representative images of the 2D gel electrophoresis are shown in Supplementary Figure 1B.

Other proteins identified by this proteomic approach have been published previously [11, 13]. A list of all regulated proteins is shown in Supplementary Table 2.

Confirmation of surgery-associated reduction in mucosal mHMGCS and ketone body levels

Western blotting confirmed the decrease of mHMGCS using the same samples that were used for the global proteomics analysis (Figure 1A; one sample from the proteomic analysis had to be omitted due to insufficient remaining volume). Blotting-analysis was performed on the confirmatory patient cohort showing similar reduction after RYGB (Figure 1B). Characteristics for all cohorts are shown in Table 1. Jejunal mucosal levels of the ketone body βHB were measured in perioperative samples from fasting patients undergone a two-week preoperative VLCD, and the same patients 6-8 months after RYGB. The postoperative levels were found to be significantly decreased (Figure 1C; peri-RYGB vs. post-RYGB; mean±SEM; 70.5±4.7 vs. 39.3±2.2 µM/µg protein, n=11; $P<0.001$; one sample had to be omitted due to technical difficulties).

mHMGCS is localized to the surface epithelial layer in human jejunum

To study mHMGCS expression morphologically we performed immunostaining of samples taken peri- and postoperatively after RYGB (n=5 sample pairs, randomly selected from confirmatory cohort). mHMGCS-immunostaining was localised to the epithelium, indicating predominant expression in enterocytes. Six months after RYGB, the immunoreactivity to mHMGCS was low or absent in all investigated specimens, thus supporting the semi-quantitative results from the proteomic and blotting-analyses. Figures 1D to 1G show representative images of peri- and postoperative staining of mHMGCS in one of the patients.

Reduction in mucosal mHMGCS is specific to surgery and is not decreased by preoperative very-low-calorie diet

Blotting-analysis of mucosa samples retrieved from diet cohort before very-low-calorie diet, at surgery and after surgery confirmed that reduction of mHMGCS was specific to surgery (Figure 2A; pre-VLCD vs. post-VLCD/peri-RYGB vs. post-RYGB; mean±SEM; 1.53±0.18 vs. 1.32±0.19 vs. 0.31±0.06; n=12). Analysis of lipid metabolism markers CPT1A (Figure 2B; mean±SEM; 0.91±0.11 vs. 1.49±0.15 vs. 0.83±0.09; n=12), FATP4 (Figure 2C; mean±SEM; 0.82±0.11 vs. 1.38±0.16 vs. 1.00±0.10; n=12) and DGAT1 (Figure 2D; mean±SEM; 0.67±0.15 vs. 2.24±0.33 vs. 0.51±0.09; n=12) revealed no change comparing samples retrieved before diet and after surgery, but an increased expression after VLCD. The ketone body utilizing enzyme SCOT was increased after VLCD but no change was seen after surgery compared to baseline (Figure 2E; baseline vs. VLCD vs. RYGB; mean±SEM; 0.93±0.08 vs. 1.49±0.19 vs. 0.77±0.08; n=12).

Mouse intestinal mHMGCS expression is fat sensitive and most pronounced in the jejunum

To confirm the induction and further investigate the potential functionality of small intestinal mucosal mHMGCS protein, animal studies were employed. C57bl/6J mice were fed either HFD or LFD over 3 weeks. HFD mice showed significantly higher weight gain compared to LFD mice (body weight gain LFD vs. HFD; mean±SEM; 0.94±0.23 vs. 5.84±0.53 g, n=8, P<0.001). Western blotting of mHMGCS was performed on specimens from the mucosa of the duodenum, the jejunum and the ileum, as well as liver. No difference in mHMGCS expression was observed in the duodenum when comparing mice on HFD and LFD (Figure 3A; LFD vs. HFD; mean±SEM; 1.10±0.23 vs. 1.35±0.18, n=6, P=NS). However, the mHMGCS protein expression observed in the jejunum (Figure 3B; LFD vs. HFD; mean±SEM; 0.59±0.03 vs. 1.43±0.20, n=5, P<0.01) and ileum (Figure 3C; LFD vs. HFD;

mean±SEM; 0.84±0.06 vs. 1.18±0.09, n=6, P<0.05) was significantly higher after HFD than LFD. A comparison of mHMGCS expression between the jejunum and the ileum revealed substantially higher levels of mHMGCS expression in the jejunum after HFD (Figure 3D; jejunum vs. ileum; mean±SEM; 1.39±0.13 vs. 0.70±0.06, n=5/6, P<0.01). mHMGCS expression in the liver was somewhat increased (Figure 3E; LFD vs. HFD; mean±SEM; 0.87±0.04 vs. 1.15±0.07, n=6, P<0.01).

Intralipid gavage in HFD-fed mice results in elevated ketone levels in portal blood

In order to examine the functionality of mHMGCS expression induced by HFD in mouse jejunum, we assessed βHB levels in portal and peripheral venous blood. C57bl/6J mice were fed either HFD or LFD during 3 months to robustly induce mHMGCS expression. After oral gavage with intralipid to the mice, venous blood was sampled at different times from the tail (Figure 3F). HFD mice showed increased βHB levels after 120 min compared to LFD mice (Figure 3G; LFD + intralipid vs. HFD + intralipid; mean±SEM; 0.50±0.08 vs. 0.87±0.10 mM, n=7, P<0.05). This increase was absent in HFD mice given the mHMGCS inhibitor hymeglusin in the oral gavage (Figure 3G; HFD + intralipid vs. HFD + intralipid + hymeglusin; mean±SEM; 0.87±0.10 vs. 0.46±0.06 mM, n=7, P<0.01). For mice fed LFD no major increase in βHB levels could be seen 120 min after the oral gavage with intralipid, not even with addition of exogenous βHB in the oral gavage (Figure 3G; LFD + intralipid + βHB vs. HFD + intralipid; mean±SEM; 0.36±0.08 vs. 0.87±0.10 mM, n=8/7, P<0.01). In another experiment, we examined βHB levels in portal vs. peripheral venous blood in mice that were fed LFD or HFD for 3 weeks. Mice fed HFD had significantly higher baseline levels of βHB in the portal vein when normalized to levels in peripheral blood (portal/peripheral blood) in contrast to LFD mice (Figure 3H; LFD portal/peripheral vs. HFD portal/peripheral; mean±SEM; 0.62±0.04 vs. 1.02±0.10, n=9, P<0.01), showing that the predominant source of

βHB shifted between LFD and HFD; with a higher proportion originating from the intestine rather than the liver. In the HFD animals, the absolute levels of βHB in portal blood were also significantly higher compared to the LFD fed animals (Figure 3I; LFD portal vs. HFD portal; mean±SEM; 1.35±0.14 vs. 3.82±0.89 mM, n=9, P<0.05); whereas there was no significant difference in the peripheral blood levels (Figure 3I; LFD peripheral vs. HFD peripheral; mean±SEM; 2.20±0.22 vs. 3.47±0.65 mM, n=9, P=NS). In the LFD animals, βHB levels were significantly lower in portal blood compared to peripheral blood (Figure 3I; LFD peripheral vs. LFD portal; mean±SEM; 2.20±0.22 vs. 1.35±0.14 mM, n=9, P<0.01), which was not the case in the HFD animals (Figure 3I; HFD peripheral vs. HFD portal; mean±SEM; 3.47±0.65 vs. 3.82±0.89 mM, n=9, P=NS). These data indicate that the difference between LFD and HFD feeding was increased intestinal, rather than decreased hepatic production of βHB.

Ketone bodies inhibit glucose-stimulated GLP-1 release from mouse small intestinal EECs

There are two known fatty acid/ketone receptors expressed on small intestinal EECs. FFAR3/GPR41, that is preferentially expressed on small intestinal human and mouse EECs, and GPR109a, which is expressed at much lower levels [14, 15]. Therefore, we tested whether ketone bodies could have effects on the release of gut peptides from EECs. Primary cultures from mouse jejunum were used to measure the effect of βHB on basal and glucose- and IBMX-stimulated release of the gut peptide GLP-1. The βHB levels were chosen based on an approximated molar concentration of βHB in human jejunal mucosa (Figure 1C). The mucosa was assumed to constitute a third of the 6 µl cylindrical volume of a 2 mm forceps biopsy sample, diluted in buffer to 30 µl in the βHB assay, thus representing a total 15-time dilution. Average measured βHB levels in the jejunal samples was 0.8 mM. At a 15-time dilution this should reflect a tissue concentration of about 12 mM *in vivo*. We decided to use βHB at a

10mM concentration, and found this to inhibit the glucose/IBMX-stimulated GLP-1 release by 43% (Figure 4A; IG + 10 mM βHB vs. IG compared to Basal). Somatostatin had an even greater inhibitory effect and completely blocked the stimulation induced by glucose/IBMX (Figure 4A). As FFAR3 and GPR109a are $G_{\alpha i}$ coupled receptors, we tested whether the blocking effect of βHB was mediated via $G_{\alpha i}$ signalling by treating the cell cultures with PTX. PTX treatment ablated the inhibitory effect of βHB on GLP-1 release in response to glucose/IBMX-stimulation (Figure 4B). PTX also blocked the effect of somatostatin, as expected (Figure 4B). Whilst these data do not specifically prove FFAR3 to mediate the inhibitory action of βHB, they do indicate the involvement of a $G_{\alpha i}$ coupled receptor.

A proposed mechanistic model

Figure 5 shows a proposed mechanistic model for how high-fat diet dose-dependently may inhibit glucose-stimulated release of gut peptides, e. g. GLP-1 from EECs. Chronic fat exposure induces increased mHMGCS expression and ketogenesis in jejunal epithelial cells (as suggested in Figures 3B, 3F to I and 1C). Ketone bodies (βHB) reach the EECs in a paracellular fashion and via the microcirculation of villi and act on FFAR3 to inhibit the release of GLP-1 (as suggested in Figure 4). RYGB surgery may inhibit this mechanism by immediately removing accessibility of FFA as substrate for ketogenesis, and by down-regulating mHMGCS expression and βHB in the jejunum (as shown in Figures 1A to C), thereby alleviating the inhibitory effect of ketone bodies on EEC incretin production.

DISCUSSION

Very few reports are available on the expression of the rate-limiting ketogenic enzyme mHMGCS in human small intestinal mucosa [16]. We show that RYGB surgery *per se*, and

not decreased caloric intake, resulted in a substantial decrease in mHMGCS expression and jejunal ketone body levels. The decreased expression and ketone body production after surgery could be caused by several different reasons, e. g. substrate unavailability caused by decreased lipolysis due to the deviation of bile/pancreatic lipases from the alimentary limb, or by increased lipid utilization for anabolic purposes or lipid oxidation for energy demand, following the hypertrophy that occurs in the alimentary limb of the jejunum after RYGB [5, 17, 18].

Ketone bodies are known to be liver-produced during starvation or high-fat low-carbohydrate ketogenic diet in order to supply energy for peripheral tissues, including the brain, when glucose levels are low. Ketogenesis has an association to short fatty acids like butyrate, which both induce mHMGCS expression via PPARα and also act as precursor substrates via β-oxidation [16]. In the small intestine mHMGCS instead has a *food intake related expression*. It has previously been shown to be highly expressed in the early postnatal period in suckling rodents, and starvation decreased its expression, in opposition to hepatic ketogenesis [19, 20]. After weaning to low-fat diet the expression disappeared from the intestine [20]. It is probably the high fat-content of breast milk that induces mHMGCS. Small intestinal expression of mHMGCS can also be re-activated by high-fat diet in adult rodents [21, 22]. Thus, intestinal ketogenesis could represent a fat-sensory mechanism of the small intestinal mucosa. It seems likely that this is a completely different nutrient-mediated signal compared to systemic ketogenesis, during which ketones have been suggested to act as systemic signaling metabolites that may *protect* against insulin resistance and type-2 diabetes [23].

In animal experiments, we confirmed that expression of mHMGCS was substantially increased in the jejunum after HFD-feeding. This expression lead to increased levels of the

ketone body βHB in the portal blood of mice. Furthermore, the βHB production was completely blocked by per-oral pretreatment with the specific mHMGCS-inhibitor hymeglusin. The local levels of ketone bodies at the site of production, i.e. the mucosal epithelial cells and in the microcirculation of villi may however be substantially higher (approximated by our mucosal measurements ~10 mM), since portal blood is "diluted" by venous return from regions of the intestine other than the jejunum. A potential limitation of our study is that it was not possible to obtain postprandial samples for ketone body measurement in RYGB-operated patients. It was recently shown that the postprandial fatty acid uptake and oxidation was increased (and not decreased) in RYGB-operated rats [18]. Whether this reflects a compensatory increase in other parts of the intestine, remains to be investigated.

The cessation of inhibitory ketone bodies on EECs could contribute to an increased gut peptide responsiveness after RYGB surgery. In cell culture on primary EECs, the ketone body βHB inhibited glucose-stimulated GLP-1 release by ~40% compared to baseline. This inhibition was mediated by a $G_{\alpha i}$ coupled receptor as it was completely reversed by the $G_{\alpha i}$ coupled receptor-inhibitor PTX. The $G_{\alpha i}$ coupled ketone body/fatty acid receptor FFAR3/GPR41 is expressed in the small intestinal epithelium, where it is highly enriched in EECs [14, 15]. It has earlier been demonstrated to be involved in the regulation of energy homeostasis, via e.g. PYY and GLP-1 [24]. Our data suggest a new mechanism, as the $G_{\alpha i}$ coupled receptor-inhibitor PTX blocked the suppressive effect of both βHB and somatostatin on GLP-1 release from EECs. However, we could not definitely conclude whether the βHB induced inhibition of GLP-1 secretion is mediated by FFAR3, or an alternative $G_{\alpha i}$ coupled receptor such as GPR109a, in the EECs. GPR109a is however expressed at a much lower level in EECs [15].

In summary, we suggest a surgical physiological reconstruction of the alimentary limb by inducing substrate deficiency for ketogenesis. This could contribute to the explanation of the very rapid improvement of incretin hormone secretion observed after RYGB, as we have recently shown is evident already two days after surgery [3]. These findings are consistent with the proposed "anti-incretin" and "foregut exclusion" hypotheses that could explain the effects of RYGB surgery on improved satiety and glucose homeostasis [10]. This may open up a new avenue for the development of anti-obesity and anti-diabetic drugs, targeting mHMGCS and intestinal mucosal ketone production, in order to increase EEC responsiveness and gut peptide release on nutrient stimulation.

ACKNOWLEDGEMENTS

We want to thank Professor Claes Ohlsson for critical reading of the manuscript. The proteomics analysis was performed at the Proteomics Core Facility, Sahlgrenska Academy, University of Gothenburg. Animal experiments in Gothenburg were performed in collaboration with and at the Centre for Physiology and Bio-Imaging (CPI), Sahlgrenska Academy, University of Gothenburg. tGLP1 immunoassays were performed at the Addenbrooke's Hospital Core Biochemical Assay Laboratory. This study was funded by the following grants: ALFGBG-673931 from the Western Region of Sweden, grants from Erik and Lily Philipson memorial foundation, MRC [MRC_MC_UU_12012/3 and MRC_MC_UU_12012/5], Wellcome Trust [106262/Z/14/Z, 106263/Z/14/Z, 100574/Z/12/Z].

COMPETING INTERESTS

Competing interest: VW reports grants from Western Region of Sweden, grants from Erik and Lily Philipson memorial foundation. FMG is a paid consultant for Kallyope, New York.

The Gribble-Reimann lab hosts projects which receive funding from Medimmune/AstraZeneca (FMG / FR). CLR reports research grants from Science Foundation Ireland, and the Health Research Board, Ireland, during the conduct of the study; other from Novo Nordisk, other from GI Dynamics, personal fees from Eli Lilly, grants and personal fees from Johnson and Johnson, personal fees from Sanofi Aventis, personal fees from Astra Zeneca, personal fees from Janssen, personal fees from Bristol-Myers Squibb, personal fees from Boehringer-Ingelheim outside of the submitted work.

REFERENCES

1. Puzziferri N, Roshek TB, 3rd, Mayo HG, Gallagher R, Belle SH, Livingston EH. Long-term follow-up after bariatric surgery: a systematic review. JAMA. 2014;312(9):934-42. doi: 10.1001/jama.2014.10706. PubMed PMID: 25182102; PubMed Central PMCID: PMCPMC4409000.
2. Rubino F, Schauer PR, Kaplan LM, Cummings DE. Metabolic surgery to treat type 2 diabetes: clinical outcomes and mechanisms of action. Annu Rev Med. 2010;61:393-411. doi: 10.1146/annurev.med.051308.105148. PubMed PMID: 20059345.
3. Wallenius V, Dirinck E, Fandriks L, Maleckas A, le Roux CW, Thorell A. Glycemic Control after Sleeve Gastrectomy and Roux-En-Y Gastric Bypass in Obese Subjects with Type 2 Diabetes Mellitus. Obes Surg. 2017. Epub 2017/12/22. doi: 10.1007/s11695-017-3061-3. PubMed PMID: 29264780.
4. Cavin JB, Voitellier E, Cluzeaud F, Kapel N, Marmuse JP, Chevallier JM, et al. Malabsorption and intestinal adaptation after one anastomosis gastric bypass compared with Roux-en-Y gastric bypass in rats. Am J Physiol Gastrointest Liver Physiol. 2016;311(3):G492-500. doi: 10.1152/ajpgi.00197.2016. PubMed PMID: 27418681.
5. Spak E, Bjorklund P, Helander HF, Vieth M, Olbers T, Casselbrant A, et al. Changes in the mucosa of the Roux-limb after gastric bypass surgery. Histopathology. 2010;57(5):680-8. doi: 10.1111/j.1365-2559.2010.03677.x. PubMed PMID: 21054493.
6. Baud G, Daoudi M, Hubert T, Raverdy V, Pigeyre M, Hervieux E, et al. Bile Diversion in Roux-en-Y Gastric Bypass Modulates Sodium-Dependent Glucose Intestinal Uptake. Cell Metab. 2016;23(3):547-53. doi: 10.1016/j.cmet.2016.01.018. PubMed PMID: 26924216.
7. Cavin JB, Couvelard A, Lebtahi R, Ducroc R, Arapis K, Voitellier E, et al. Differences in Alimentary Glucose Absorption and Intestinal Disposal of Blood Glucose After Roux-en-Y Gastric Bypass vs Sleeve Gastrectomy. Gastroenterology. 2016;150(2):454-64 e9. doi: 10.1053/j.gastro.2015.10.009. PubMed PMID: 26481855.
8. Saeidi N, Meoli L, Nestoridi E, Gupta NK, Kvas S, Kucharczyk J, et al. Reprogramming of intestinal glucose metabolism and glycemic control in rats after gastric bypass. Science. 2013;341(6144):406-10. doi: 10.1126/science.1235103. PubMed PMID: 23888041; PubMed Central PMCID: PMCPMC4068965.

9. Makinen J, Hannukainen JC, Karmi A, Immonen HM, Soinio M, Nelimarkka L, et al. Obesity-associated intestinal insulin resistance is ameliorated after bariatric surgery. Diabetologia. 2015;58(5):1055-62. doi: 10.1007/s00125-015-3501-3. PubMed PMID: 25631620; PubMed Central PMCID: PMCPMC4392118.
10. Salinari S, Mingrone G, Bertuzzi A, Previti E, Capristo E, Rubino F. Downregulation of Insulin Sensitivity After Oral Glucose Administration: Evidence for the Anti-Incretin Effect. Diabetes. 2017;66(11):2756-63. doi: 10.2337/db17-0234. PubMed PMID: 28851712.
11. Casselbrant A, Elias E, Fandriks L, Wallenius V. Expression of tight-junction proteins in human proximal small intestinal mucosa before and after Roux-en-Y gastric bypass surgery. Surg Obes Relat Dis. 2015;11(1):45-53. Epub 2014/09/30. doi: 10.1016/j.soard.2014.05.009. PubMed PMID: 25264329.
12. Psichas A, Tolhurst G, Brighton CA, Gribble FM, Reimann F. Mixed Primary Cultures of Murine Small Intestine Intended for the Study of Gut Hormone Secretion and Live Cell Imaging of Enteroendocrine Cells. J Vis Exp. 2017;(122). doi: 10.3791/55687. PubMed PMID: 28448057; PubMed Central PMCID: PMCPMC5409300.
13. Elias E, Casselbrant A, Werling M, Abegg K, Vincent RP, Alaghband-Zadeh J, et al. Bone mineral density and expression of vitamin D receptor-dependent calcium uptake mechanisms in the proximal small intestine after bariatric surgery. Br J Surg. 2014;101(12):1566-75. Epub 2014/09/12. doi: 10.1002/bjs.9626. PubMed PMID: 25209438.
14. Nohr MK, Pedersen MH, Gille A, Egerod KL, Engelstoft MS, Husted AS, et al. GPR41/FFAR3 and GPR43/FFAR2 as cosensors for short-chain fatty acids in enteroendocrine cells vs FFAR3 in enteric neurons and FFAR2 in enteric leukocytes. Endocrinology. 2013;154(10):3552-64. doi: 10.1210/en.2013-1142. PubMed PMID: 23885020.
15. Roberts GP, Larraufie P, Richards P, Kay RG, Galvin SG, Miedzybrodzka EL, et al. Comparison of Human and Murine Enteroendocrine Cells by Transcriptomic and Peptidomic Profiling. Diabetes. 2019;68(5):1062-72. doi: 10.2337/db18-0883. PubMed PMID: 30733330; PubMed Central PMCID: PMCPMC6477899.
16. Wang Q, Zhou Y, Rychahou P, Fan TW, Lane AN, Weiss HL, et al. Ketogenesis contributes to intestinal cell differentiation. Cell Death Differ. 2017;24(3):458-68. Epub 2016/12/10. doi: 10.1038/cdd.2016.142. PubMed PMID: 27935584; PubMed Central PMCID: PMCPMC5344206.
17. Hansen CF, Bueter M, Theis N, Lutz T, Paulsen S, Dalboge LS, et al. Hypertrophy dependent doubling of L-cells in Roux-en-Y gastric bypass operated rats. PLoS One. 2013;8(6):e65696. doi: 10.1371/journal.pone.0065696. PubMed PMID: 23776529; PubMed Central PMCID: PMCPMC3679162.
18. Kaufman S, Arnold M, Diaz AA, Neubauer H, Wolfrum S, Kofeler H, et al. Roux-en-Y gastric bypass surgery reprograms enterocyte triglyceride metabolism and postprandial secretion in rats. Mol Metab. 2019;23:51-9. doi: 10.1016/j.molmet.2019.03.002. PubMed PMID: 30905616; PubMed Central PMCID: PMCPMC6480308.
19. Bekesi A, Williamson DH. An explanation for ketogenesis by the intestine of the suckling rat: the presence of an active hydroxymethylglutaryl-coenzyme A pathway. Biol Neonate. 1990;58(3):160-5. doi: 10.1159/000243256. PubMed PMID: 2279051.
20. Thumelin S, Forestier M, Girard J, Pegorier JP. Developmental changes in mitochondrial 3-hydroxy-3-methylglutaryl-CoA synthase gene expression in rat liver, intestine and kidney. Biochem J. 1993;292 (Pt 2):493-6. PubMed PMID: 8099282; PubMed Central PMCID: PMCPMC1134236.
21. Clara R, Schumacher M, Ramachandran D, Fedele S, Krieger JP, Langhans W, et al. Metabolic Adaptation of the Small Intestine to Short- and Medium-Term High-Fat Diet

Exposure. J Cell Physiol. 2017;232(1):167-75. doi: 10.1002/jcp.25402. PubMed PMID: 27061934.
22. de Wit NJ, Boekschoten MV, Bachmair EM, Hooiveld GJ, de Groot PJ, Rubio-Aliaga I, et al. Dose-dependent effects of dietary fat on development of obesity in relation to intestinal differential gene expression in C57BL/6J mice. PLoS One. 2011;6(4):e19145. doi: 10.1371/journal.pone.0019145. PubMed PMID: 21547079; PubMed Central PMCID: PMCPMC3081848.
23. Ramachandran D, Clara R, Fedele S, Hu J, Lackzo E, Huang JY, et al. Intestinal SIRT3 overexpression in mice improves whole body glucose homeostasis independent of body weight. Mol Metab. 2017;6(10):1264-73. doi: 10.1016/j.molmet.2017.07.009. PubMed PMID: 29031725; PubMed Central PMCID: PMCPMC5641632.
24. Inoue D, Tsujimoto G, Kimura I. Regulation of Energy Homeostasis by GPR41. Front Endocrinol (Lausanne). 2014;5:81. doi: 10.3389/fendo.2014.00081. PubMed PMID: 24904531; PubMed Central PMCID: PMCPMC4033597.

FIGURE LEGENDS

Figure 1.

Western blot analysis of jejunal mHMGCS protein expression peri- and post-RYGB. (A) Upper panel shows Western blots of mHMGCS in jejunal samples from the proteomics cohort of patients (n=6). Neighboring samples represent pairs of peri- (white bars above) and postoperative (grey bars above) samples from the same patient. GAPDH was used as loading control and is shown below each corresponding mHMGCS band. Lower panel shows densitometric measurement of mHMGCS normalized to GAPDH (arbitrary densitometric units; ADU) peri- and post-RYGB. (B) Upper panel shows Western blot of mHMGCS in jejunal samples from the confirmatory cohort of RYGB patients peri- and post-RYGB (n=9). Group pairs originating from multiple Western blots were merged for presentation of all pairs. Lower panel shows densitometric measurement of mHMGCS normalized to GAPDH (ADU; arbitrary densitometric units) peri- and post-RYGB. (C) measurement of the ketone body βHB in human jejunal mucosa samples after a two-week preoperative VLCD and 6-8 months postoperatively after RYGB surgery in the same patients (n=11). (D) mHMGCS-immunofluorescence from one patient perioperatively and (E) 6 months postoperatively after RYGB. (F) and (G) show corresponding hematoxylin & eosin stainings to panels (D) and (E), respectively. Statistical analyses were performed using Wilcoxon signed-rank test where * indicates $P<0.05$, ** $P<0.01$, *** $P<0.001$. +ve=positive control.

Figure 2. Western blot analyses of jejunal mHMGCS, and several fat-metabolism associated proteins pre-VLCD, post-VLCD/peri-RYGB and post-RYGB from the diet cohort of patients (n=12). The upper panels show Western blots of (A) mHMGCS, (B) CPT1A, (C) FATP4, (D) DGAT1 and (E) the ketone body-utilizing enzyme SCOT. In each panel representative protein bands from three of the patients for the protein of interest and the corresponding loading

control GAPDH are shown. Neighboring samples represent pre-VLCD (white bars above Western blots), post-VLCD/peri-RYGB (grey bars) and post-RYGB (black bars) samples from the same patient. In the lower panels expression of each protein of interest has been normalized to the loading control GAPDH and is presented in the bar graphs (ADU; arbitrary densitometric units). Statistical analyses were performed using Wilcoxon signed-rank test where * indicates $P<0.05$, ** $P<0.01$ and *** $P<0.001$.

Figure 3. Western blot analyses of the effects of low-fat diet (LFD; white bars above blots) vs. high-fat diet (HFD; grey bars above blots) on mHMGCS protein expression. Upper panels show mHMGCS expression in (A) duodenum, (B) jejunum, (C) ileum, (D) jejunum vs. ileum and (E) liver in C57bl/6J mice on LFD or HFD. GAPDH was used as loading control and is shown below each corresponding mHMGCS band. Lower panels show the corresponding densitometric quantifications (ADU; arbitrary densitometric units) of mHMGCS vs. GAPDH. Note that (D) shows comparison of mHMGCS in the jejunum (light grey bar) vs. ileum (dark grey bar) in HFD fed mice to demonstrate the difference in expression levels between jejunum and ileum. (F) measurement of βHB at 0, 15, 30 and 120 min in venous blood of mice fed LFD or HFD for 3 months. Prior to the experiment the mice were given an oral fat load (250 µl of Intralipid®) in order to supply substrate for ketogenesis. In some mice the oral fat load was mixed with βHB, or the mHMGCS-inhibitor hymeglusin, as indicated. (G) shows the measurements from (F) at 120 min in a scatter plot (n=7-8). βHB levels in venous blood were significantly higher in the HFD mice 120 min after oral gavage compared to LFD mice. Notably, the βHB levels in HFD mice pretreated with the mHMGCS-inhibitor hymeglusin did not increase. (H) mice fed HFD for 3 weeks had significantly higher levels of ketone bodies in portal vein blood normalized to ketone bodies in peripheral blood, in contrast to mice fed LFD (n=9) after oral gavage with Intralipid® (500 µl). (I) absolute levels of ketone bodies

(mM) in peripheral and portal blood in the same mice as in panel H (n=9). Statistical analyses were performed using Mann-Whitney U-test where * indicates $P<0.05$ and ** $P<0.01$.

Figure 4. (A) normalized GLP-1 levels in unstimulated (basal, 1mM glucose) mouse jejunal primary cultures (first cluster from the left), after stimulation with 10 mM glucose/0.1 mM IBMX (IG; second from left), or a combination of 10 mM glucose/0.1 mM IBMX and 10 mM βHB (third from left), or a combination of 10 mM glucose/0.1 mM IBMX and 0.1 μM somatostatin (fourth from left). (B) same group setup as A, but all groups were also treated with 500 ng/mL PTX in order to block $G\alpha_i$ signaling. The different symbols depict replicates of jejunal primary cultures. Statistical analyses were performed using two-way ANOVA followed by Tukey's HSD-test where * indicates $P<0.05$, ** $P<0.01$ and *** $P<0.001$.

Figure 5. Schematic illustration of the proposed ketone body mechanism on GLP-1 producing enteroendocrine cells (EECs). Chronic FFA exposure induces increased mHMGCS expression and βHB production in jejunal epithelial cells in the villi tips. βHB reaches the EECs via the venous microcirculation of the villi, and acts via FFAR3/GPR41 to inhibit the production/release of GLP-1. RYGB surgery may interfere with this mechanism by decreasing FFA availability and mHMGCS expression.

Supplementary Figure 1.

(A) the sampling sites of the jejunal mucosa peri- and postoperatively after RYGB (left and right panels, respectively).

(B) example of 2D-gel electrophoresis obtained perioperatively (left panel) and postoperatively (right panel) from one individual. Examples of spots with changed intensities are encircled by white rectangles and highlighted in the lower panels by the green circles and

numbered according to software identification numbers. Mass spectrometry identification of these proteins is shown in Supplementary Table 2. Spots 1660, 1670 & 1678 represent postoperatively decreased mHMGCS.

Supplementary Table 1. Primary and secondary antibodies used for Western blotting and immunofluorescence.

Primary antibody	Manufacturer	Catalog number	Application
mHMGCS	Santa Cruz Bio.	sc-33828	Western blot and immunofluorescence
CPT1A	Abcam	ab128568	Western blot
FATP4	Atlas Antibodies	HPA007293	Western blot
DGAT1	Santa Cruz Bio.	sc-271934	Western blot
SCOT	Santa Cruz Bio.	sc-133988	Western blot
GAPDH	Imgenex	IMG-5143A	Western blot
GAPDH	Novus Biologicals	NB100-56875	Western blot
Secondary antibody	**Manufacturer**	**Catalog number**	**Application**
Goat anti-rabbit IgG-AP	Santa Cruz Bio.	sc-2007	Western blot
Anti-mouse IgG HRP-linked	Cell Signaling	7076	Western blot
Anti-rabbit IgG HRP-linked	Cell Signaling	7074	Western blot
Alexa Fluor 488 goat anti-rabbit	ThermoFisher Sci.	A11008	Immunofluorescence

Supplementary Table 2. Paired analysis of 2D-gels peri- and 6 to 8 months postoperatively and identification of corresponding proteins with tandem mass spectrometry.

Spot Id.	Spot cluster Id.	Accession number[a)]	Gene/Protein designation	Protein description	Protein score[b)]	Change	Paired t-test
2838	8	Q01995	TAGLN	Transgelin	611	-2.4	<0.001
2754	7	P30626	SRI	Sorcin	301	-1.6	0.018
2093	6	P09493	TPM1	Tropomyosin alpha-1 chain	852	-1.6	0.013
2050	6	P09493	TPM1	Tropomyosin alpha-1 chain	1338	-1.6	0.010
1988	6	P07951	TPM2	Tropomyosin beta chain	1121	-1.6	0.024
1678	5	P54868	mHMGCS	Hydroxymethylglutaryl-CoA synthase, mitochondrial	558	-3.6	<0.001
1670	5	P41240	mHMGCS	Hydroxymethylglutaryl-CoA synthase, mitochondrial	577	-3.6	<0.001
1661	5	P41240	mHMGCS	Hydroxymethylglutaryl-CoA synthase, mitochondrial	530	-2.2	<0.001
1660	5	P54868	mHMGCS	Hydroxymethylglutaryl-CoA synthase, mitochondrial	652	-4.0	<0.001
1646	4	P05783	KRT18	Keratin, type I cytoskeletal 18	673	-2.2	<0.001
1640	4	P05783	KRT18	Keratin, type 1 cytoskeletal 18	1029	+1.9	0.008
1627	4	P35900	KRT20	Keratin, type I cytoskeletal 20	1852	+2.0	0.004
1606	4	P35900	KRT20	Keratin, type I cytoskeletal 20	1539	+1.7	0.011
1605	4	P05787	KRT8	Keratin, type II cytoskeletal 8	1226	+2.0	0.033
1603	4	P05787	KRT8	Keratin, type II cytoskeletal 8	1166	+1.8	0.027
1594	4	P05787	KRT8	Keratin, type II cytoskeletal 8	1324	+1.9	0.032
1459	4	P05787	KRT8	Keratin, type II cytoskeletal 8	2026	+1.9	0.002
1441	4	P05787	KRT8	Keratin, type II cytoskeletal 8	1872	+2.1	0.003
1432	4	P05787	KRT8	Keratin, type II cytoskeletal 8	1942	+1.7	0.038
1427	4	P05787	KRT8	Keratin, type II cytoskeletal 8	1567	+2.2	0.004
1421	4	P05787	KRT8	Keratin, type II cytoskeletal 8	1675	+2.0	0.015
935	3	P08238	HSP90AB1	Heat shock protein HSP 90-β	450	-1.6	0.006
478	1	P12109	COL6A1	Collagen alpha-1(VI) chain	701	-1.7	0.002
469	1	P12109	COL6A1	Collagen alpha-1(VI) chain	797	-1.9	0.004
431	2	P18206	VCL	Vinculin	884	-1.7	0.021
420	2	P18206	VCL	Vinculin	1100	-1.8	0.010
416	2	P18206	VCL	Vinculin	1018	-1.7	0.018

a) Accession number in Uniprot database
b) Protein match score in Mascot search results

Figure 1

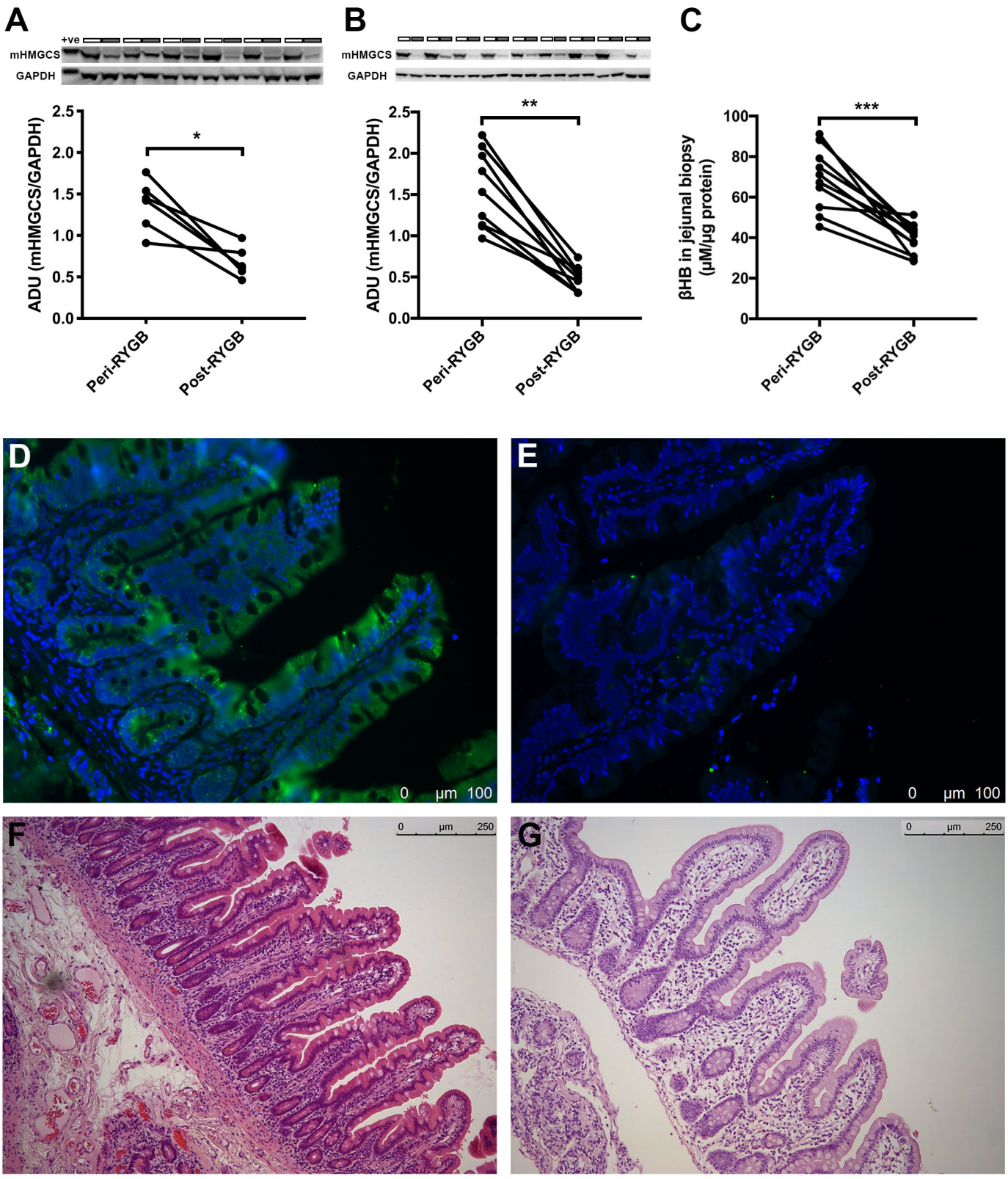
A
+ve
mHMGCS
GAPDH
ADU (mHMGCS/GAPDH)
2.5
2.0
1.5
1.0
0.5
0.0
*
Peri-RYGB
Post-RYGB
B
mHMGCS
GAPDH
ADU (mHMGCS/GAPDH)
**
Peri-RYGB
Post-RYGB
C
βHB in jejunal biopsy (μM/μg protein)
100
80
60
40
20
0
***
Peri-RYGB
Post-RYGB
D
0 μm 100
E
0 μm 100
F
0 μm 250
G
0 μm 250

Figure 2

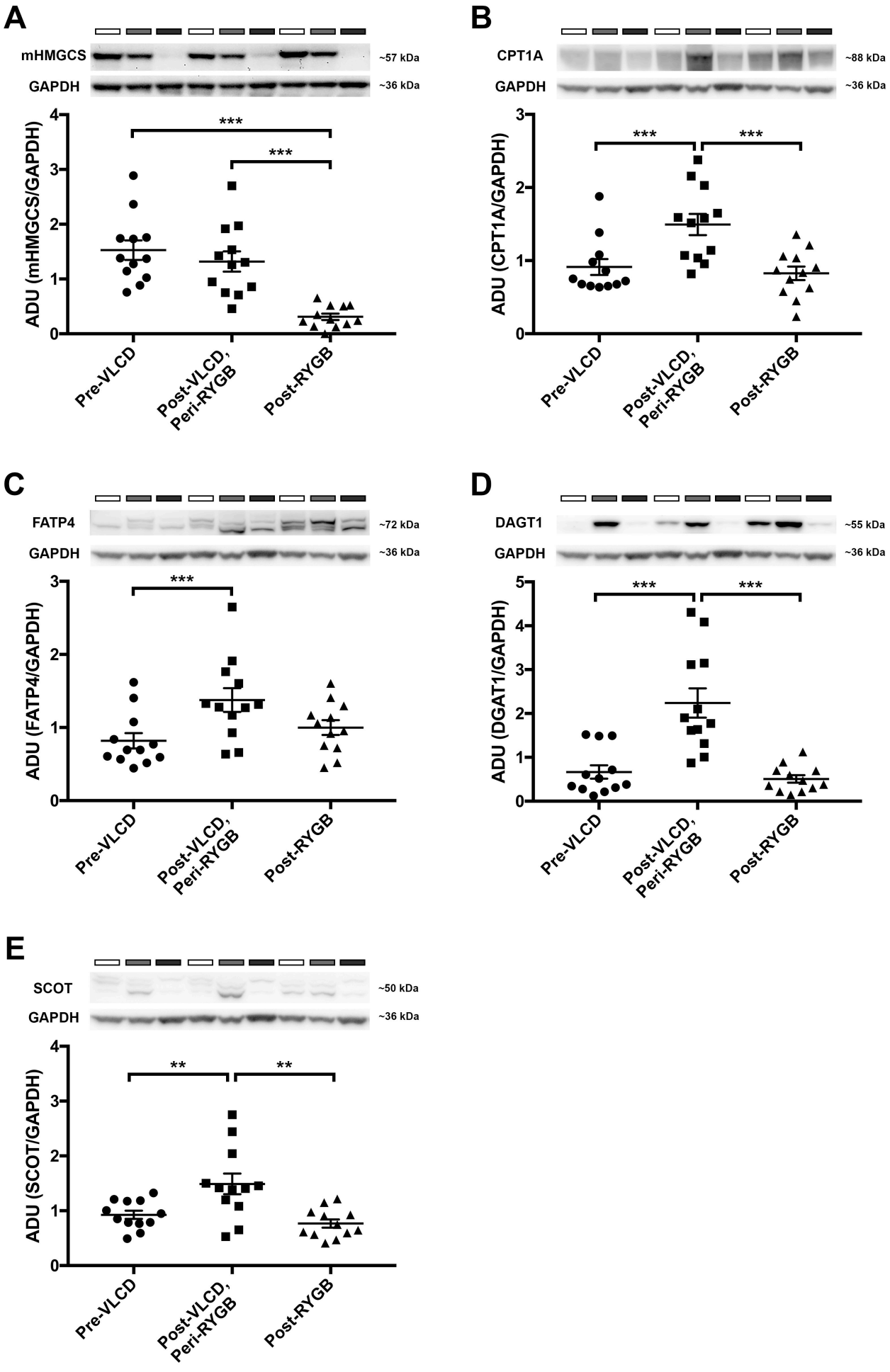
A
mHMGCS
~57 kDa
GAPDH
~36 kDa
ADU (mHMGCS/GAPDH)
***
***
Pre-VLCD
Post-VLCD, Peri-RYGB
Post-RYGB
B
CPT1A
~88 kDa
GAPDH
~36 kDa
ADU (CPT1A/GAPDH)
***
***
Pre-VLCD
Post-VLCD, Peri-RYGB
Post-RYGB
C
FATP4
~72 kDa
GAPDH
~36 kDa
ADU (FATP4/GAPDH)
***
Pre-VLCD
Post-VLCD, Peri-RYGB
Post-RYGB
D
DAGT1
~55 kDa
GAPDH
~36 kDa
ADU (DGAT1/GAPDH)
***
***
Pre-VLCD
Post-VLCD, Peri-RYGB
Post-RYGB
E
SCOT
~50 kDa
GAPDH
~36 kDa
ADU (SCOT/GAPDH)
**
**
Pre-VLCD
Post-VLCD, Peri-RYGB
Post-RYGB

Figure 3

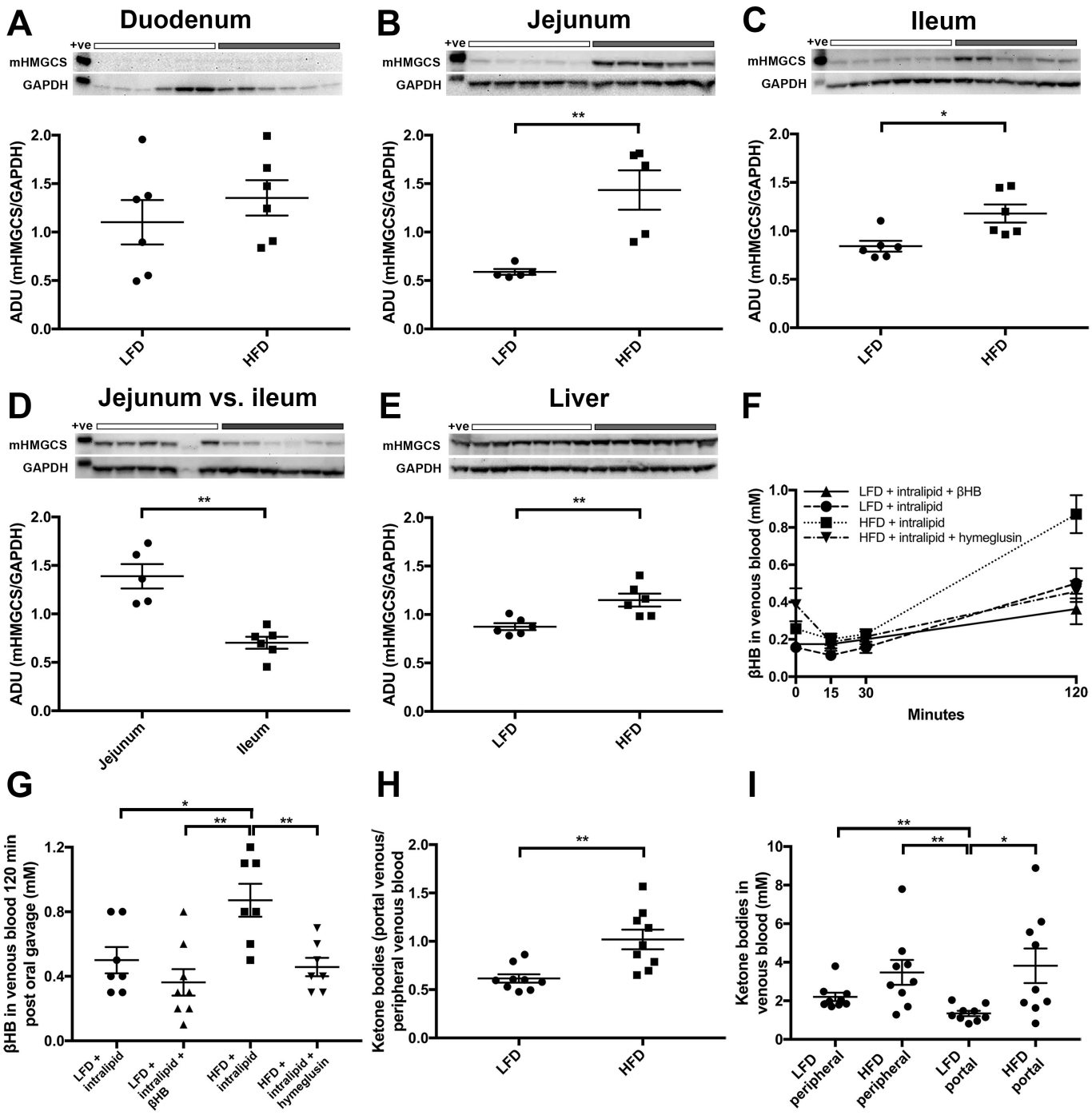
A
Duodenum
+ve
mHMGCS
GAPDH
ADU (mHMGCS/GAPDH)
LFD
HFD
B
Jejunum
C
Ileum
D
Jejunum vs. ileum
Jejunum
Ileum
E
Liver
F
LFD + intralipid + βHB
LFD + intralipid
HFD + intralipid
HFD + intralipid + hymeglusin
βHB in venous blood (mM)
Minutes
G
βHB in venous blood 120 min post oral gavage (mM)
LFD + intralipid
LFD + intralipid + βHB
HFD + intralipid
HFD + intralipid + hymeglusin
H
Ketone bodies (portal venous/ peripheral venous blood
I
Ketone bodies in venous blood (mM)
LFD peripheral
HFD peripheral
LFD portal
HFD portal

Figure 4

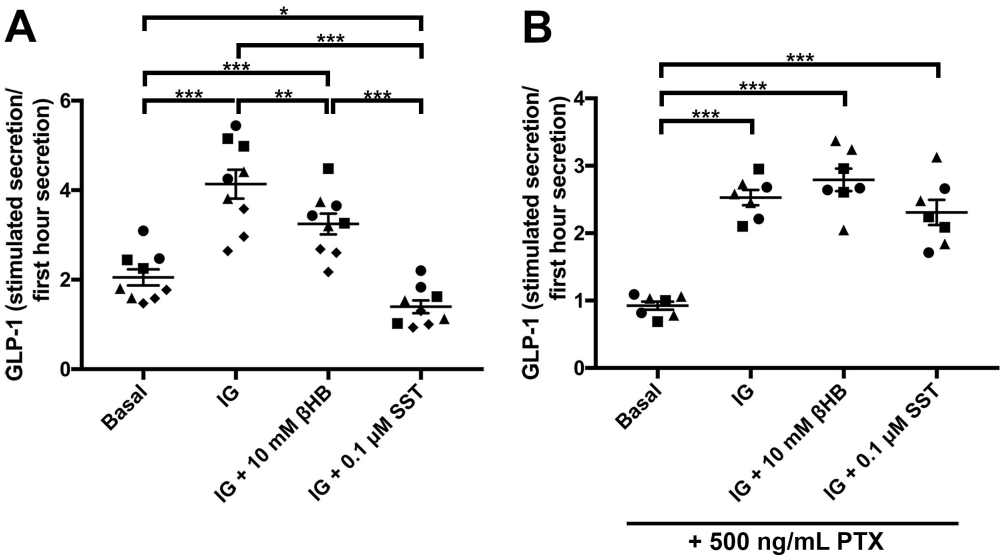
A
B
GLP-1 (stimulated secretion/ first hour secretion)
Basal
IG
IG + 10 mM βHB
IG + 0.1 μM SST
+ 500 ng/mL PTX
*
***
**

Figure 5

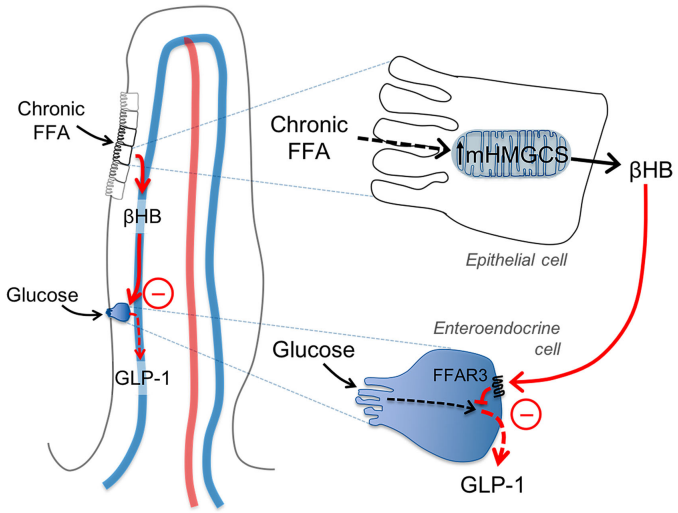
Chronic
FFA
βHB
Glucose
GLP-1
Chronic
FFA
↑mHMGCS
βHB
Epithelial cell
Enteroendocrine
cell
Glucose
FFAR3
GLP-1

Supplementary Figure 1